

Measurement of exclusive $B \rightarrow X_u \ell \nu$ decays using a full-reconstruction tag at Belle

K. Abe,⁹ K. Abe,⁴⁹ I. Adachi,⁹ H. Aihara,⁵¹ D. Anipko,¹ K. Aoki,²⁵ T. Arakawa,³²
K. Arinstein,¹ Y. Asano,⁵⁶ T. Aso,⁵⁵ V. Aulchenko,¹ T. Aushev,²¹ T. Aziz,⁴⁷ S. Bahinipati,⁴
A. M. Bakich,⁴⁶ V. Balagura,¹⁵ Y. Ban,³⁷ S. Banerjee,⁴⁷ E. Barberio,²⁴ M. Barbero,⁸
A. Bay,²¹ I. Bedny,¹ K. Belous,¹⁴ U. Bitenc,¹⁶ I. Bizjak,¹⁶ S. Blyth,²⁷ A. Bondar,¹
A. Bozek,³⁰ M. Bračko,^{23,16} J. Brodzicka,^{9,30} T. E. Browder,⁸ M.-C. Chang,⁵⁰ P. Chang,²⁹
Y. Chao,²⁹ A. Chen,²⁷ K.-F. Chen,²⁹ W. T. Chen,²⁷ B. G. Cheon,³ R. Chistov,¹⁵
J. H. Choi,¹⁸ S.-K. Choi,⁷ Y. Choi,⁴⁵ Y. K. Choi,⁴⁵ A. Chuvikov,³⁹ S. Cole,⁴⁶ J. Dalseno,²⁴
M. Danilov,¹⁵ M. Dash,⁵⁷ R. Dowd,²⁴ J. Dragic,⁹ A. Drutskoy,⁴ S. Eidelman,¹ Y. Enari,²⁵
D. Epifanov,¹ S. Fratina,¹⁶ H. Fujii,⁹ M. Fujikawa,²⁶ N. Gabyshev,¹ A. Garmash,³⁹
T. Gershon,⁹ A. Go,²⁷ G. Gokhroo,⁴⁷ P. Goldenzweig,⁴ B. Golob,^{22,16} A. Gorišek,¹⁶
M. Grosse Perdekamp,^{11,40} H. Guler,⁸ H. Ha,¹⁸ J. Haba,⁹ K. Hara,²⁵ T. Hara,³⁵
Y. Hasegawa,⁴⁴ N. C. Hastings,⁵¹ K. Hayasaka,²⁵ H. Hayashii,²⁶ M. Hazumi,⁹
D. Heffernan,³⁵ T. Higuchi,⁹ L. Hinz,²¹ T. Hokuue,²⁵ Y. Hoshi,⁴⁹ K. Hoshina,⁵⁴ S. Hou,²⁷
W.-S. Hou,²⁹ Y. B. Hsiung,²⁹ Y. Igarashi,⁹ T. Iijima,²⁵ K. Ikado,²⁵ A. Imoto,²⁶ K. Inami,²⁵
A. Ishikawa,⁵¹ H. Ishino,⁵² K. Itoh,⁵¹ R. Itoh,⁹ M. Iwabuchi,⁶ M. Iwasaki,⁵¹ Y. Iwasaki,⁹
C. Jacoby,²¹ M. Jones,⁸ H. Kakuno,⁵¹ J. H. Kang,⁵⁸ J. S. Kang,¹⁸ P. Kapusta,³⁰
S. U. Kataoka,²⁶ N. Katayama,⁹ H. Kawai,² T. Kawasaki,³² H. R. Khan,⁵² A. Kibayashi,⁵²
H. Kichimi,⁹ N. Kikuchi,⁵⁰ H. J. Kim,²⁰ H. O. Kim,⁴⁵ J. H. Kim,⁴⁵ S. K. Kim,⁴³
T. H. Kim,⁵⁸ Y. J. Kim,⁶ K. Kinoshita,⁴ N. Kishimoto,²⁵ S. Korpar,^{23,16} Y. Kozakai,²⁵
P. Križan,^{22,16} P. Krokovny,⁹ T. Kubota,²⁵ R. Kulasiri,⁴ R. Kumar,³⁶ C. C. Kuo,²⁷
E. Kurihara,² A. Kusaka,⁵¹ A. Kuzmin,¹ Y.-J. Kwon,⁵⁸ J. S. Lange,⁵ G. Leder,¹³ J. Lee,⁴³
S. E. Lee,⁴³ Y.-J. Lee,²⁹ T. Lesiak,³⁰ J. Li,⁸ A. Limosani,⁹ C. Y. Lin,²⁹ S.-W. Lin,²⁹
Y. Liu,⁶ D. Liventsev,¹⁵ J. MacNaughton,¹³ G. Majumder,⁴⁷ F. Mandl,¹³ D. Marlow,³⁹
T. Matsumoto,⁵³ A. Matyja,³⁰ S. McOnie,⁴⁶ T. Medvedeva,¹⁵ Y. Mikami,⁵⁰ W. Mitaroff,¹³
K. Miyabayashi,²⁶ H. Miyake,³⁵ H. Miyata,³² Y. Miyazaki,²⁵ R. Mizuk,¹⁵ D. Mohapatra,⁵⁷
G. R. Moloney,²⁴ T. Mori,⁵² J. Mueller,³⁸ A. Murakami,⁴¹ T. Nagamine,⁵⁰ Y. Nagasaka,¹⁰
T. Nakagawa,⁵³ Y. Nakahama,⁵¹ I. Nakamura,⁹ E. Nakano,³⁴ M. Nakao,⁹ H. Nakazawa,⁹
Z. Natkaniec,³⁰ K. Neichi,⁴⁹ S. Nishida,⁹ K. Nishimura,⁸ O. Nitoh,⁵⁴ S. Noguchi,²⁶
T. Nozaki,⁹ A. Ogawa,⁴⁰ S. Ogawa,⁴⁸ T. Ohshima,²⁵ T. Okabe,²⁵ S. Okuno,¹⁷ S. L. Olsen,⁸
S. Ono,⁵² W. Ostrowicz,³⁰ H. Ozaki,⁹ P. Pakhlov,¹⁵ G. Pakhlova,¹⁵ H. Palka,³⁰
C. W. Park,⁴⁵ H. Park,²⁰ K. S. Park,⁴⁵ N. Parslow,⁴⁶ L. S. Peak,⁴⁶ M. Pernicka,¹³
R. Pestotnik,¹⁶ M. Peters,⁸ L. E. Piilonen,⁵⁷ A. Poluektov,¹ F. J. Ronga,⁹ N. Root,¹
J. Rorie,⁸ M. Rozanska,³⁰ H. Sahoo,⁸ S. Saitoh,⁹ Y. Sakai,⁹ H. Sakamoto,¹⁹ H. Sakaue,³⁴
T. R. Sarangi,⁶ N. Sato,²⁵ N. Satoyama,⁴⁴ K. Sayeed,⁴ T. Schietinger,²¹ O. Schneider,²¹
P. Schönmeier,⁵⁰ J. Schümann,²⁸ C. Schwanda,¹³ A. J. Schwartz,⁴ R. Seidl,^{11,40} T. Seki,⁵³
K. Senyo,²⁵ M. E. Sevier,²⁴ M. Shapkin,¹⁴ Y.-T. Shen,²⁹ H. Shibuya,⁴⁸ B. Shwartz,¹
V. Sidorov,¹ J. B. Singh,³⁶ A. Sokolov,¹⁴ A. Somov,⁴ N. Soni,³⁶ R. Stamen,⁹ S. Stanić,³³
M. Starić,¹⁶ H. Stoeck,⁴⁶ A. Sugiyama,⁴¹ K. Sumisawa,⁹ T. Sumiyoshi,⁵³ S. Suzuki,⁴¹
S. Y. Suzuki,⁹ O. Tajima,⁹ N. Takada,⁴⁴ F. Takasaki,⁹ K. Tamai,⁹ N. Tamura,³²

K. Tanabe,⁵¹ M. Tanaka,⁹ G. N. Taylor,²⁴ Y. Teramoto,³⁴ X. C. Tian,³⁷ I. Tikhomirov,¹⁵
 K. Trabelsi,⁹ Y. T. Tsai,²⁹ Y. F. Tse,²⁴ T. Tsuboyama,⁹ T. Tsukamoto,⁹ K. Uchida,⁸
 Y. Uchida,⁶ S. Uehara,⁹ T. Uglov,¹⁵ K. Ueno,²⁹ Y. Unno,⁹ S. Uno,⁹ P. Urquijo,²⁴
 Y. Ushiroda,⁹ Y. Usov,¹ G. Varner,⁸ K. E. Varvell,⁴⁶ S. Villa,²¹ C. C. Wang,²⁹
 C. H. Wang,²⁸ M.-Z. Wang,²⁹ M. Watanabe,³² Y. Watanabe,⁵² J. Wicht,²¹ L. Widhalm,¹³
 J. Wiechczynski,³⁰ E. Won,¹⁸ C.-H. Wu,²⁹ Q. L. Xie,¹² B. D. Yabsley,⁴⁶ A. Yamaguchi,⁵⁰
 H. Yamamoto,⁵⁰ S. Yamamoto,⁵³ Y. Yamashita,³¹ M. Yamauchi,⁹ Heyoung Yang,⁴³
 S. Yoshino,²⁵ Y. Yuan,¹² Y. Yusa,⁵⁷ S. L. Zang,¹² C. C. Zhang,¹² J. Zhang,⁹
 L. M. Zhang,⁴² Z. P. Zhang,⁴² V. Zhilich,¹ T. Ziegler,³⁹ A. Zupanc,¹⁶ and D. Zürcher²¹

(The Belle Collaboration)

¹*Budker Institute of Nuclear Physics, Novosibirsk*

²*Chiba University, Chiba*

³*Chonnam National University, Kwangju*

⁴*University of Cincinnati, Cincinnati, Ohio 45221*

⁵*University of Frankfurt, Frankfurt*

⁶*The Graduate University for Advanced Studies, Hayama*

⁷*Gyeongsang National University, Chinju*

⁸*University of Hawaii, Honolulu, Hawaii 96822*

⁹*High Energy Accelerator Research Organization (KEK), Tsukuba*

¹⁰*Hiroshima Institute of Technology, Hiroshima*

¹¹*University of Illinois at Urbana-Champaign, Urbana, Illinois 61801*

¹²*Institute of High Energy Physics,*

Chinese Academy of Sciences, Beijing

¹³*Institute of High Energy Physics, Vienna*

¹⁴*Institute of High Energy Physics, Protvino*

¹⁵*Institute for Theoretical and Experimental Physics, Moscow*

¹⁶*J. Stefan Institute, Ljubljana*

¹⁷*Kanagawa University, Yokohama*

¹⁸*Korea University, Seoul*

¹⁹*Kyoto University, Kyoto*

²⁰*Kyungpook National University, Taegu*

²¹*Swiss Federal Institute of Technology of Lausanne, EPFL, Lausanne*

²²*University of Ljubljana, Ljubljana*

²³*University of Maribor, Maribor*

²⁴*University of Melbourne, Victoria*

²⁵*Nagoya University, Nagoya*

²⁶*Nara Women's University, Nara*

²⁷*National Central University, Chung-li*

²⁸*National United University, Miao Li*

²⁹*Department of Physics, National Taiwan University, Taipei*

³⁰*H. Niewodniczanski Institute of Nuclear Physics, Krakow*

³¹*Nippon Dental University, Niigata*

³²*Niigata University, Niigata*

³³*University of Nova Gorica, Nova Gorica*

³⁴*Osaka City University, Osaka*

³⁵*Osaka University, Osaka*

- ³⁶*Panjab University, Chandigarh*
³⁷*Peking University, Beijing*
³⁸*University of Pittsburgh, Pittsburgh, Pennsylvania 15260*
³⁹*Princeton University, Princeton, New Jersey 08544*
⁴⁰*RIKEN BNL Research Center, Upton, New York 11973*
⁴¹*Saga University, Saga*
⁴²*University of Science and Technology of China, Hefei*
⁴³*Seoul National University, Seoul*
⁴⁴*Shinshu University, Nagano*
⁴⁵*Sungkyunkwan University, Suwon*
⁴⁶*University of Sydney, Sydney NSW*
⁴⁷*Tata Institute of Fundamental Research, Bombay*
⁴⁸*Toho University, Funabashi*
⁴⁹*Tohoku Gakuin University, Tagajo*
⁵⁰*Tohoku University, Sendai*
⁵¹*Department of Physics, University of Tokyo, Tokyo*
⁵²*Tokyo Institute of Technology, Tokyo*
⁵³*Tokyo Metropolitan University, Tokyo*
⁵⁴*Tokyo University of Agriculture and Technology, Tokyo*
⁵⁵*Toyama National College of Maritime Technology, Toyama*
⁵⁶*University of Tsukuba, Tsukuba*
⁵⁷*Virginia Polytechnic Institute and State University, Blacksburg, Virginia 24061*
⁵⁸*Yonsei University, Seoul*

Abstract

We report a preliminary study of the branching fractions and q^2 distributions of exclusive charmless semileptonic B decays, using events tagged by fully reconstructing one of the B mesons in a hadronic decay mode. These results are obtained from a data sample that contains 535×10^6 $B\bar{B}$ pairs, collected near the $\Upsilon(4S)$ resonance with the Belle detector at the KEKB asymmetric energy e^+e^- collider.

PACS numbers: 13.25.Hw, 13.30.Ce, 14.40.Nd

The Standard Model (SM) of particle physics contains a number of parameters whose values are not predicted by theory and must therefore be measured by experiment. In the quark sector, the elements of the Cabibbo-Kobayashi-Maskawa (CKM) matrix govern the weak transitions between quark flavours, and precision measurements of their values are desirable. In particular, much experimental and theoretical effort is currently being employed to test the consistency of the CKM formalism [1], by examining the Unitarity Triangle most relevant to the decays of B mesons.

The precision to which the angle $\sin 2\phi_1$ characterising indirect CP violation in $b \rightarrow c\bar{c}s$ transitions has improved to approximately 5% [2]. This makes a precision measurement of the length of the side of the Unitarity triangle opposite to ϕ_1 particularly important as a consistency check of the SM picture. The length of this side is determined to good approximation by the ratio of the magnitudes of two CKM matrix elements, $|V_{ub}|/|V_{cb}|$. Both of these can be measured using exclusive semileptonic B meson decays. Using charmed semileptonic decays, the precision to which $|V_{cb}|$ has been determined is of order 2%. On the other hand $|V_{ub}|$, which can be measured using charmless semileptonic decays, is the most poorly known of the CKM matrix elements. Both inclusive and exclusive methods of measuring $|V_{ub}|$ have been pursued, with the inclusive methods giving a value to a precision of 7-8%. The exclusive determination of $|V_{ub}|$ currently has a precision poorer than 10%. It is the aim of an ongoing programme of measurements at the B factories to improve this precision to better than 5%, for comparison with the inclusive results, which have somewhat different experimental and theoretical systematics. This would provide a sharp consistency test with the value of $\sin 2\phi_1$.

In this paper we present preliminary studies of the exclusive semileptonic decays $B \rightarrow \pi^+\ell\nu$, $B \rightarrow \pi^0\ell\nu$, $B \rightarrow \rho^+\ell\nu$, $B \rightarrow \rho^0\ell\nu$ and $B \rightarrow \omega\ell\nu$ using a full reconstruction tagging technique to identify candidate B mesons. This measurement is based on a data sample that contains $535 \times 10^6 B\bar{B}$ pairs, collected with the Belle detector at the KEKB asymmetric-energy e^+e^- (3.5 on 8 GeV) collider [3]. KEKB operates at the $\Upsilon(4S)$ resonance ($\sqrt{s} = 10.58$ GeV) with a peak luminosity that exceeds $1.6 \times 10^{34} \text{ cm}^{-2}\text{s}^{-1}$. The $\Upsilon(4S)$ is produced with a Lorentz boost of $\beta\gamma = 0.425$ nearly along the electron beamline (z).

The Belle detector is a large-solid-angle magnetic spectrometer that consists of a silicon vertex detector (SVD), a 50-layer central drift chamber (CDC), an array of aerogel threshold Čerenkov counters (ACC), a barrel-like arrangement of time-of-flight scintillation counters (TOF), and an electromagnetic calorimeter comprised of CsI(Tl) crystals (ECL) located inside a super-conducting solenoid coil that provides a 1.5 T magnetic field. An iron flux-return located outside of the coil is instrumented to detect K_L^0 mesons and to identify muons (KLM). The detector is described in detail elsewhere [4]. Two inner detector configurations were used. A 2.0 cm beampipe and a 3-layer silicon vertex detector was used for the first sample of $152 \times 10^6 B\bar{B}$ pairs, while a 1.5 cm beampipe, a 4-layer silicon detector and a small-cell inner drift chamber were used to record the remaining $383 \times 10^6 B\bar{B}$ pairs[5].

Table I lists all current measurements of branching fractions for exclusive $B \rightarrow X_u\ell\nu$ decays, where X_u denotes a light meson containing a u quark. This table is based on a recent compilation by the Heavy Flavour Averaging Group (HFAG) [6]. Three methods of identifying signal candidates have been employed in these measurements, denoted “untagged”, “semileptonic tagged” or “full reconstruction tagged”. Only BaBar have reported results to date based on the third of these [12] [14].

The most precise measurements at the present time come from the untagged analyses of CLEO [7] and BaBar [8]. As more integrated luminosity is accumulated by the B -factory

experiments, the full reconstruction tagging technique will become the most precise method. It holds the advantage of providing the best signal to background ratio, offset by the lowest efficiencies.

TABLE I: Measurements of branching fractions of exclusive $B \rightarrow X_u \ell \nu$ decay modes. In each case, the first error is statistical, the second experimental systematic, the third due to form factor uncertainties for the signal mode, and the fourth, when present, due to form factor uncertainties for crossfeed modes. U indicates untagged method, S semileptonic tagging method, and F full reconstruction tagging.

| Experiment and Tag Method | | Mode | $B\bar{B}$ [10^6] | Branching Fraction [10^{-4}] |
|------------------------------|---|-----------------------------------|--------------------------|---|
| CLEO [7] | U | $B^0 \rightarrow \pi^- \ell \nu$ | 9.7 | $1.33 \pm 0.18 \pm 0.11 \pm 0.01 \pm 0.07$ |
| BaBar [8] | U | $B^0 \rightarrow \pi^- \ell \nu$ | 86 | $1.38 \pm 0.10 \pm 0.16 \pm 0.08$ |
| Belle [9] | S | $B^0 \rightarrow \pi^- \ell \nu$ | 275 | $1.38 \pm 0.19 \pm 0.14 \pm 0.03$ |
| Belle [9] | S | $B^+ \rightarrow \pi^0 \ell \nu$ | 275 | $0.77 \pm 0.14 \pm 0.08 \pm 0.00$ |
| BaBar [10] | S | $B^0 \rightarrow \pi^- \ell \nu$ | 232 | $1.03 \pm 0.25 \pm 0.13$ |
| BaBar [11] | S | $B^+ \rightarrow \pi^0 \ell \nu$ | 88 | $1.80 \pm 0.37 \pm 0.23$ |
| BaBar [12] | F | $B^0 \rightarrow \pi^- \ell \nu$ | 233 | $1.14 \pm 0.27 \pm 0.17$ |
| BaBar [12] | F | $B^+ \rightarrow \pi^0 \ell \nu$ | 233 | $0.86 \pm 0.22 \pm 0.11$ |
| BaBar [12] | F | $B \rightarrow \pi \ell \nu$ | 233 | $1.28 \pm 0.23 \pm 0.16$ |
| CLEO [7] | U | $B^0 \rightarrow \rho^- \ell \nu$ | 9.7 | $2.17 \pm 0.34^{+0.47}_{-0.54} \pm 0.41 \pm 0.01$ |
| CLEO [13] | U | $B^0 \rightarrow \rho^- \ell \nu$ | 3.3 | $2.69 \pm 0.41^{+0.35}_{-0.40} \pm 0.50$ |
| BaBar [14] | F | $B^0 \rightarrow \rho^- \ell \nu$ | 88 | $2.57 \pm 0.52 \pm 0.59$ |
| BaBar [15] | U | $B^0 \rightarrow \rho^- e \nu$ | 55 | $3.29 \pm 0.42 \pm 0.47 \pm 0.60$ |
| BaBar [8] | U | $B^0 \rightarrow \rho^- \ell \nu$ | 83 | $2.14 \pm 0.21 \pm 0.51 \pm 0.28$ |
| Belle [9] | S | $B^0 \rightarrow \rho^- \ell \nu$ | 275 | $2.17 \pm 0.54 \pm 0.31 \pm 0.08$ |
| Belle [9] | S | $B^+ \rightarrow \rho^0 \ell \nu$ | 275 | $1.33 \pm 0.23 \pm 0.17 \pm 0.05$ |
| Belle [16] | U | $B^+ \rightarrow \omega \ell \nu$ | 85 | $1.3 \pm 0.4 \pm 0.2 \pm 0.3$ |
| CLEO [7] | U | $B^+ \rightarrow \eta \ell \nu$ | 9.7 | $0.84 \pm 0.31 \pm 0.16 \pm 0.09$ |

In this analysis we fully reconstruct one of the two B mesons from the $\Upsilon(4S)$ decay (B_{tag}) in one of the following hadronic decay modes, $B^- \rightarrow D^{(*)0} \pi^-$, $B^- \rightarrow D^{(*)0} \rho^-$, $B^- \rightarrow D^{(*)0} a_1^-$, $B^- \rightarrow D^{(*)0} D_s^{*-}$, $B^0 \rightarrow D^{(*)+} \pi^-$, $B^0 \rightarrow D^{(*)+} \rho^-$, $B^0 \rightarrow D^{(*)+} a_1^-$ or $B^0 \rightarrow D^{(*)+} D_s^{*-}$ [17]. Decays are identified on the basis of the proximity of the beam-energy constrained mass $M_{\text{bc}} = \sqrt{(E_{\text{beam}})^2 - (\vec{p}_B)^2}$ and $\Delta E = E_B - E_{\text{beam}}$ to their nominal values of the B meson rest mass and zero, respectively. Here E_{beam} , \vec{p}_B and E_B are the beam energy and the measured 3-momentum and energy of the B_{tag} candidate in the $\Upsilon(4S)$ rest frame respectively. If multiple tag candidates are found, the one with values of M_{bc} and ΔE closest to nominal is chosen. Events with a B_{tag} satisfying the selections $M_{\text{bc}} > 5.27 \text{ GeV}/c^2$ and $-0.08 < \Delta E < 0.06 \text{ GeV}$ are retained. The charge of the B_{tag} candidate is necessarily restricted to $Q_{\text{tag}} = 0$ or $Q_{\text{tag}} = \pm 1$ by demanding that it is consistent with one of the above decay modes.

Reconstructed charged tracks and ECL clusters which are not associated with the B_{tag} candidate are used to search for the signal B meson decays of interest recoiling against the

B_{tag} . Photons identified with isolated ECL clusters which have a laboratory energy of less than 50 MeV are ignored.

Electrons are identified using information on dE/dx from the CDC, response of the ACC, shower shape in the ECL, and the ratio of the energy deposited in the ECL to the momentum determined from tracking. The signals in the KLM are used to identify muons. Charged kaons are identified based on the dE/dx information from the CDC, the Čerenkov light yields in the ACC and time-of-flight information from the TOF counters. Any charged particles which are not identified as leptons or kaons are taken to be pions.

Photons whose direction in the laboratory frame lies within a 5° cone of the direction of an identified lepton are considered to be bremsstrahlung. The 4-momentum of the photon is added to that of the lepton and the photon is not considered further.

Neutral pions are reconstructed from pairs of photons whose invariant mass lies in the range $[0.120, 0.150]$ GeV/ c^2 , of order $\pm 3\sigma$ of the π^0 mass. Charged ρ meson candidates are reconstructed via the decay $\rho^\pm \rightarrow \pi^\pm \pi^0$ where the invariant mass of the pair of pions is required to lie in the range $[0.570, 0.970]$ GeV/ c^2 . Neutral ρ meson candidates are similarly reconstructed from pairs of oppositely charged pions, with the requirement that $m_{\pi^+\pi^-}$ is in the range $[0.703, 0.863]$ GeV/ c^2 . Finally, ω candidates are reconstructed from $\omega \rightarrow \pi^+\pi^-\pi^0$ with $m_{\pi^+\pi^-\pi^0}$ in the range $[0.690, 0.850]$ GeV/ c^2 . In events where more than one hadron candidate, denoted X_u , of a given type is identified amongst the recoil particles, the candidate with the highest momentum in the $\Upsilon(4S)$ rest frame is chosen.

To isolate signal candidates, several requirements are placed on the recoil system. There must be one lepton candidate present only, with $p_{\text{lep}} > 0.4$ GeV/ c in the $\Upsilon(4S)$ rest frame. The total charge of the recoil system, Q_{recoil} , is required to be 0 if a neutral tag has been identified, and ± 1 if a charged tag has been identified. In the charged case, the sign of Q_{recoil} must be opposite to that of Q_{tag} . In the neutral case, we do not make any requirement on the sign of the lepton charge with respect to the B_{tag} , to allow for mixing.

The number of charged recoil particles is required to correspond to one of the sought modes, i.e. one for $B \rightarrow \pi^0 \ell \nu$ (the lepton), two for $B \rightarrow \pi^+ \ell \nu$ and $B \rightarrow \rho^+ \ell \nu$ (the lepton plus one charged pion) and three for $B \rightarrow \rho^0 \ell \nu$ and $B \rightarrow \omega \ell \nu$ (the lepton plus two charged pions). Additionally, the number of recoil π^0 candidates is required to be consistent with one of the sought modes. In order to increase efficiency, however, we allow more than the necessary number in some cases: we require no π^0 candidates to be present for $B \rightarrow \pi^+ \ell \nu$ and $B \rightarrow \rho^0 \ell \nu$ modes, and at least one π^0 for the $B \rightarrow \pi^0 \ell \nu$, $B \rightarrow \rho^+ \ell \nu$ and $B \rightarrow \omega \ell \nu$ modes. Additionally, we require that there be no more than 0.3 GeV of residual neutral energy present on the recoil side in the $\Upsilon(4S)$ rest frame, after any photons contributing to the X_u candidate have been removed.

Signal events are identified by examining the missing mass squared (M_{miss}^2) distributions. If the tagging B is correctly reconstructed and the correct lepton and hadron candidate have been identified on the recoil side, then (ideally) all missing 4-momentum is due to the remaining unidentified neutrino. The square of the missing 4-momentum for signal events should therefore be close to zero, and applying this requirement provides a very strong discrimination between signal and background.

Background contributions come from several sources. These include semileptonic decays resulting from $b \rightarrow c \ell \nu$ transitions, denoted $B \rightarrow X_c \ell \nu$, which have significantly larger branching fractions to the channels under study; continuum $e^+ + e^- \rightarrow q\bar{q}$ processes; and cross feed from one $B \rightarrow X_u \ell \nu$ channel into another. The contributions of these backgrounds are studied using Monte Carlo (MC) simulated data samples generated with the EvtGeb

package [18]. Generic $B\bar{B}$ and continuum MC samples equivalent to approximately twice the integrated luminosity of the real data set are used. The model adopted for $B \rightarrow D^*\ell\nu$ and $B \rightarrow D\ell\nu$ decays is based on HQET and parametrisation of the form factors [19], while $B \rightarrow D^{**}\ell\nu$ decays are based on the ISGW2 model [20]. A non-resonant $B \rightarrow D^{(*)}\pi\ell\nu$ component based on the Goity-Roberts prescription [21] is also included.

A separate MC sample equivalent to approximately seven times the integrated luminosity of the real data set is used to simulate the signal channels and crossfeed from other $B \rightarrow X_u\ell\nu$ decays. Models for the exclusive modes are based on Light Cone Sum Rules (LSCR) for π [22], ρ and ω [23] modes and ISGW2 [20] for other exclusive modes.

Radiative effects associated with the lepton and resulting from higher-order QED processes are modelled in all MC samples using the PHOTOS package [24]. All generated MC events are passed through a full simulation of Belle detector effects based on GEANT 3.21 [25].

Figure shows the observed M_{miss}^2 distributions for the five decay modes. Also shown in this figure are the fitted signal component, the fitted $u\ell\nu$ crossfeed, and the fitted contribution from other backgrounds, which is dominated by $B \rightarrow X_c\ell\nu$ decays. The shapes of these components are taken from MC and the normalizations are fit parameters. The fitting method follows that of Barlow and Beeston [26] and takes into account finite Monte Carlo statistics. The fitted event yields obtained are 48 ± 8 for the $B \rightarrow \pi^+\ell\nu$ mode, 35 ± 7 for $B \rightarrow \pi^0\ell\nu$, 41 ± 9 for $B \rightarrow \rho^+\ell\nu$, 61 ± 9 for $B \rightarrow \rho^0\ell\nu$ and 27 ± 9 for $B \rightarrow \omega\ell\nu$.

We extract the partial branching fractions in bins of q^2 , the invariant mass squared of the lepton-neutrino system, in order to minimise the systematic error which arises from the lack of precise knowledge of the shape of the form factors. These are shown in Figure . Three bins of q^2 are chosen, commensurate with available statistics, 0 to 8 GeV^2/c^2 , 8 to 16 GeV^2/c^2 , and greater than 16 GeV^2/c^2 . The neutrino 4-momentum is determined from the missing 4-momentum vector using $p_\nu = (|\vec{p}_{\text{miss}}|, \vec{p}_{\text{miss}})$, where \vec{p}_{miss} is the missing 3-momentum vector in the $\Upsilon(4S)$ rest frame. The q^2 resolution obtained varies from 0.20 GeV^2/c^2 for the $B \rightarrow \pi^+\ell\nu$ channel to 0.27 GeV^2/c^2 for the $B \rightarrow \omega\ell\nu$ channel.

Table II summarises the result of a preliminary study of the contributions to the total systematic error for the branching fractions summed over the three q^2 bins, for the $B \rightarrow \pi^+\ell\nu$ and $B \rightarrow \pi^0\ell\nu$ modes. These are broken down into the following categories; those arising from detector simulation, such as charged track reconstruction efficiency, particle identification and neutral cluster reconstruction; uncertainties in the luminosity; and effects of the form factor models used and assumed branching fractions in the MC.

The effects of model dependence of the form factor shapes assumed in the $B \rightarrow X_u\ell\nu$ MC used for signal efficiency and crossfeed background estimates have been studied by comparing the fitted yields obtained using the default model implemented in the MC, which is LCSR [23] [22], and the ISGW2 model [20]. This is achieved by reweighting the MC events on an event-by-event basis based on their generated values of q^2 and angular variables. The variation between these two models in predicting the shapes of the q^2 distributions for the pseudoscalar and vector modes typifies the spread between available models for the dynamics of these decays.

Effects due to the uncertainties in the branching fraction normalisations for $b \rightarrow u\ell\nu$ and $b \rightarrow c\ell\nu$ decays in the signal and background MC samples were studied by varying in turn the $B \rightarrow \pi^+\ell\nu$, $B \rightarrow \pi^0\ell\nu$, $B \rightarrow \rho^+\ell\nu$, $B \rightarrow \rho^0\ell\nu$, $B \rightarrow \omega\ell\nu$, $B \rightarrow D^+\ell\nu$, $B \rightarrow D^0\ell\nu$, $B \rightarrow D^{*+}\ell\nu$ and $B \rightarrow D^{*0}\ell\nu$ branching fractions by their measurement errors as quoted by the Particle Data Group [27]. A reweighting technique is again used, and fitted yields

with and without reweighting are compared. The maximum observed spread in the fitted branching fraction is assigned as systematic error.

The effects of finite MC statistics are taken into account in the fitting procedure [26] and are reflected in the errors on the obtained branching fractions. Since the available MC samples are rather limited in statistics, variations of the assumptions on form factor shapes and normalizations can be absorbed by the present fits to a significant extent.

TABLE II: Results of a preliminary study of sources of systematic uncertainty.

| Source of error | Assigned systematic error | |
|---|--------------------------------|--------------------------------|
| | $B \rightarrow \pi^+ \ell \nu$ | $B \rightarrow \pi^0 \ell \nu$ |
| Detector Simulation: | | |
| Pion track finding eff. | 1.3% | - |
| π^0 reconstruction eff. | - | 4.6% |
| Lepton track finding eff. | 1% | 1% |
| Lepton identification | 2.1% | 2.1% |
| Charged kaon identification | 2.0% | - |
| Combined | 3.3% | 5.2% |
| $N(B\overline{B})$ uncertainty | | 1.3% |
| Form Factor Shapes: | | |
| π (LCSR \rightarrow ISGW2) | 2.2% | 1.4% |
| ρ, ω (LCSR \rightarrow ISGW2) | 0.1% | 2.4% |
| Branching Fractions: | | |
| $b \rightarrow u \ell \nu$ | 0.0% | 2.2% |
| $b \rightarrow c \ell \nu$ | 0.7% | 2.2% |
| Total systematic error | 4.2% | 6.8% |

The partial branching fractions in bins of q^2 are given in Table III for the $B \rightarrow \pi^+ \ell \nu$ and $B \rightarrow \pi^0 \ell \nu$ modes, for which reliable preliminary systematic errors have been estimated. The systematic errors are included for each bin as well as the sum over bins. Figure 2 presents the shapes of the partial branching fractions for all five modes as a function of q^2 , where the statistical and systematic errors have been added in quadrature. The systematic errors for the vector modes in this figure should be considered as very preliminary.

TABLE III: Partial branching fractions in three bins of q^2 . These are summed to give the full branching fraction quoted in the “Sum” column. Errors are statistical and systematic.

| Mode | $\Delta\mathcal{B} [10^{-4}]$ | | | $\mathcal{B} [10^{-4}]$ |
|--------------------------------|-------------------------------------|-------------------------------------|-------------------------------------|-------------------------------------|
| | $0 < q^2 < 8$ | $8 < q^2 < 16$ | $q^2 > 16$ | Sum |
| | (GeV ² /c ²) | (GeV ² /c ²) | (GeV ² /c ²) | (GeV ² /c ²) |
| $B \rightarrow \pi^+ \ell \nu$ | $0.50 \pm 0.14 \pm 0.02$ | $0.68 \pm 0.18 \pm 0.03$ | $0.31 \pm 0.12 \pm 0.01$ | $1.49 \pm 0.26 \pm 0.06$ |
| $B \rightarrow \pi^0 \ell \nu$ | $0.28 \pm 0.09 \pm 0.02$ | $0.22 \pm 0.08 \pm 0.04$ | $0.36 \pm 0.12 \pm 0.02$ | $0.86 \pm 0.17 \pm 0.06$ |

In summary, we have made a preliminary study of the partial branching fractions as a function of q^2 for five semileptonic decay channels of B mesons to charmless final states,

using a full reconstruction tag method. Summed over the three q^2 bins we obtain the following estimates of the branching fractions for the pion modes: $\mathcal{B}(B \rightarrow \pi^+ \ell \nu) = (1.49 \pm 0.26 \pm 0.06) \times 10^{-4}$, $\mathcal{B}(B \rightarrow \pi^0 \ell \nu) = (0.86 \pm 0.17 \pm 0.06) \times 10^{-4}$, where the first error is statistical and the second a preliminary estimate of the systematic error. Whilst the statistical precision of these measurements is limited at present, the potential power of the full reconstruction tagging method, when it can be used with larger accumulated B -factory data samples in the future, can clearly be seen.

We thank the KEKB group for the excellent operation of the accelerator, the KEK cryogenics group for the efficient operation of the solenoid, and the KEK computer group and the National Institute of Informatics for valuable computing and Super-SINET network support. We acknowledge support from the Ministry of Education, Culture, Sports, Science, and Technology of Japan and the Japan Society for the Promotion of Science; the Australian Research Council and the Australian Department of Education, Science and Training; the National Science Foundation of China and the Knowledge Innovation Program of the Chinese Academy of Sciences under contract No. 10575109 and IHEP-U-503; the Department of Science and Technology of India; the BK21 program of the Ministry of Education of Korea, the CHEP SRC program and Basic Research program (grant No. R01-2005-000-10089-0) of the Korea Science and Engineering Foundation, and the Pure Basic Research Group program of the Korea Research Foundation; the Polish State Committee for Scientific Research; the Ministry of Science and Technology of the Russian Federation; the Slovenian Research Agency; the Swiss National Science Foundation; the National Science Council and the Ministry of Education of Taiwan; and the U.S. Department of Energy.

-
- [1] M. Kobayashi and T. Maskawa, Prog. Theor. Phys. **49**, 652 (1973).
 - [2] For a recent review presented at FPCP06 see T. Hara, hep-ex/060507.
 - [3] S. Kurokawa and E. Kikutani, Nucl. Instr. and. Meth. **A499**, 1 (2003), and other papers included in this volume.
 - [4] A. Abashian *et al.* (Belle Collab.), Nucl. Instr. and Meth. A **479**, 117 (2002).
 - [5] Y. Ushiroda (Belle SVD2 Group), Nucl. Instr. and Meth.A **511** 6 (2003).
Z. Natkaniec *et al.*, Nucl. Instr. and Meth.A **560** 1 (2006).
 - [6] Heavy Flavor Averaging Group, <http://www.slac.stanford.edu/xorg/hfag> .
 - [7] CLEO Collaboration, S. B. Athar *et al.*, Phys. Rev. D **68**, 072003 (2003).
 - [8] BaBar Collaboration, B. Aubert *et al.*, Phys. Rev. D **72**, 051102 (2005).
 - [9] Belle Collaboration, T. Hokuue *et al.*, hep-ex/0604024.
 - [10] BaBar Collaboration, B. Aubert *et al.*, hep-ex/0506064.
 - [11] BaBar Collaboration, B. Aubert *et al.*, hep-ex/0506065.
 - [12] BaBar Collaboration, B. Aubert *et al.*, hep-ex/0507085.
 - [13] CLEO Collaboration, B. H. Behrens *et al.*, Phys. Rev. D **61**, 052001 (2000).
 - [14] BaBar Collaboration, B. Aubert *et al.*, hep-ex/0408068.
 - [15] BaBar Collaboration, B. Aubert *et al.*, Phys. Rev. D **90**, 181801 (2003).
 - [16] Belle Collaboration, C. Schwanda *et al.*, Phys. Rev. Lett. **93**, 131803 (2004).

- [17] Throughout this paper, the inclusion of the charge conjugate mode decay is implied unless otherwise stated.
- [18] D.J. Lange, Nucl. Instrum. Meth. **A462**, 152-155 (2001).
- [19] I. Caprini, L. Lellouch and M. Neubert, Nucl. Phys. **B530**, 153 (1998).
- [20] D. Scora and N. Isgur, Phys. Rev. **D 52**, 2783 (1995).
- [21] J.L. Goity and W. Roberts, Phys. Rev. **D 51**, 3459 (1995).
- [22] P. Ball and R. Zwicky, JHEP **0110**, 19 (2001).
- [23] P. Ball and V. M. Braun, Phys. Rev. D **58**, 094016 (1998).
- [24] E. Barberio and Z. Was, Comp. Phys. Commun. **79**, 291 (1994).
- [25] R. Brun *et al.* GEANT 3.21 CERN Report DD/EE/84-1, (1984).
- [26] R. Barlow and C. Beeston, Comp. Phys. Comm. **77**, 219 (1993).
- [27] W.-M. Yao *et al.* (Particle Data Group), J. Phys. **G 33**, 1 (2006).

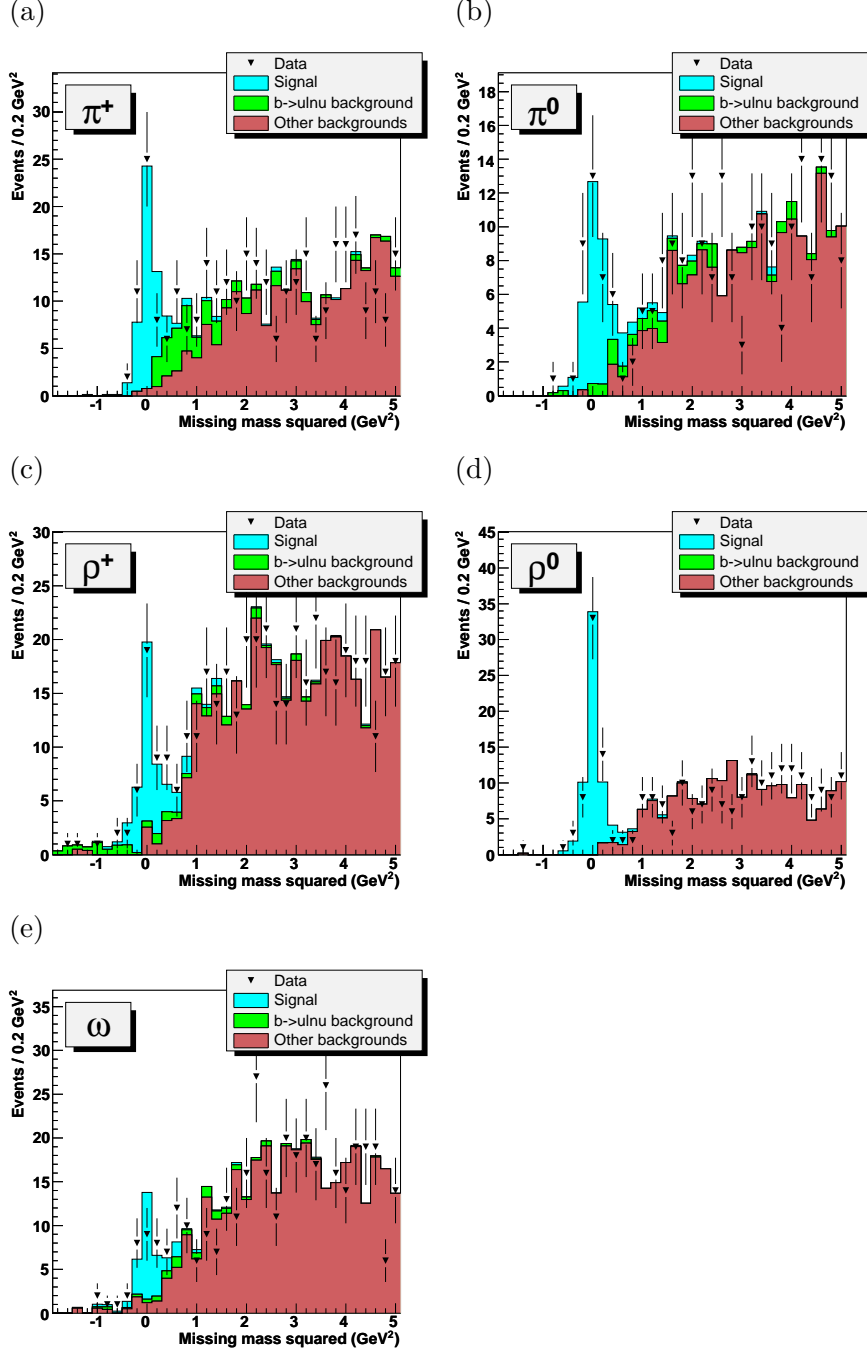


FIG. 1: Missing mass squared (M_{miss}^2) distributions after all cuts, for (a) $B \rightarrow \pi^+ \ell \nu$, (b) $B \rightarrow \pi^0 \ell \nu$, (c) $B \rightarrow \rho^+ \ell \nu$, (d) $B \rightarrow \rho^0 \ell \nu$, and (e) $B \rightarrow \omega \ell \nu$ modes. Data is indicated by the points with error bars. The blue histogram (lightest shade in greyscale) shows the fitted prediction based on the LCSR model [22] [23]. The green histogram (middle shade in greyscale) shows the fitted $b \rightarrow ul\nu$ background contribution. The crimson histogram (darkest shade in greyscale) shows the fitted background contribution from other sources. The fitting method is explained in the text.

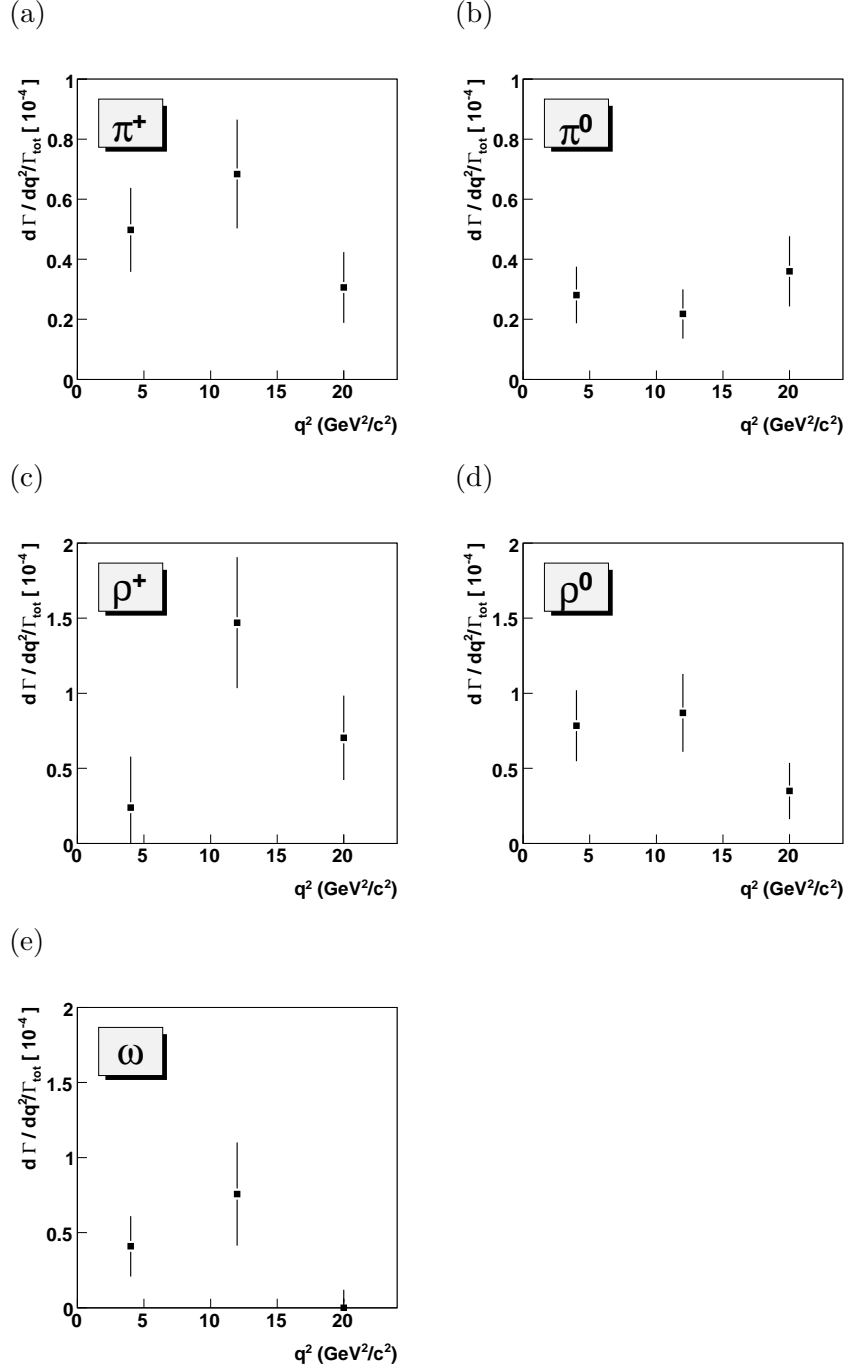


FIG. 2: Partial branching fractions as a function of q^2 for the five signal modes (a) $B \rightarrow \pi^+ \ell \nu$, (b) $B \rightarrow \pi^0 \ell \nu$, (c) $B \rightarrow \rho^+ \ell \nu$, (d) $B \rightarrow \rho^0 \ell \nu$, and (e) $B \rightarrow \omega \ell \nu$. Errors shown are statistical and preliminary systematic, added in quadrature.